

## Migration-assisted energy transfer at conjugated polymer/metal interfaces

D. E. Markov and P. W. M. Blom

*Molecular Electronics, Materials Science Centre, University of Groningen, Nijenborgh 4, NL-9747 AG Groningen, The Netherlands*

(Received 5 August 2005; published 10 October 2005)

The dynamics of exciton quenching in a conjugated polymer due to the presence of metal films is analyzed using time-resolved photoluminescence. The quenching is governed by direct radiationless energy transfer to the metal and is further enhanced by diffusion of excitons into the depletion area of the exciton population at the polymer/metal interface. The time-resolved luminescence is described by a numerical exciton diffusion model with the energy transfer incorporated via long-range dipole-dipole interaction at the metallic mirror. This allows us to disentangle the contributions from direct energy transfer to the metal and exciton migration, to the exciton quenching process. For an aluminum electrode strong exciton quenching occurs in a region of typically 15 nm, which can be decomposed in a characteristic energy-transfer range of 7.5 nm and an exciton diffusion length of 6 nm.

DOI: [10.1103/PhysRevB.72.161401](https://doi.org/10.1103/PhysRevB.72.161401)

PACS number(s): 78.20.Bh, 78.47.+p, 78.66.Qn

The application of conjugated polymers in polymer light-emitting diodes (PLEDs) and solar cells is currently attracting much attention due to easy and low-cost manufacture of these devices, their mechanical flexibility, and their light weight. In PLEDs (Refs. 1 and 2) metallic electrodes are used to inject charge carriers that subsequently form excitons. However, the presence of a metallic film allows excitons to transfer their energy nonradiatively towards the electrode, thereby lowering the efficiency of the PLED.<sup>3</sup> Also in photovoltaic devices<sup>4,5</sup> excitons formed upon photoexcitation can transfer their energy to the metallic electrodes, thereby reducing the yield of free charge-carrier production.<sup>6</sup> The effect of metal films on the photoluminescence (PL) and electroluminescence (EL) of conjugated polymers has been extensively studied using time-integrated PL.<sup>3</sup> From the dependence of the PL quantum yield on the thickness of the polymer film a typical width of the exciton quenching region can be estimated. For cyanoderivatives of poly(p-phenylene vinylene) (PPV) it has been demonstrated that both PL and EL of the polymer are strongly quenched within a typical distance of 20 nm from gold or aluminum interfaces.<sup>3</sup> The obtained characteristic quenching distance with respect to the metal interface can then be used as a measure for the effectiveness of the exciton quenching process. However, it does not discriminate between various mechanisms that contribute to the quenching process. In fact, there are two main processes that are responsible for exciton quenching by metallic films.

The first is the nonradiative energy transfer from the excited polymer to the metal via long-range dipole-dipole interaction. This process provides an extra exciton decay channel and results in an enhancement of the nonradiative decay rate close to the metal. The radiative (intrinsic) properties of the emissive species are also modified by the metal mirror due to interference effects. This has been demonstrated to be important for highly luminescent conjugated polymers;<sup>3</sup> radiative exciton lifetime modification increases with increasing luminescence quantum efficiency of the material and becomes distinct at long distances from the metal interface.<sup>7,8</sup> A detailed theory of an oscillating dipole and energy transfer near metal interfaces has been developed<sup>9,10</sup> and agreement

between experiment and theory has been demonstrated by Chance and co-workers.<sup>7,11</sup> It should be noted that for calculating the lifetime (or quantum efficiency) of the luminescence of a conjugated polymer near a metal interface additional assumptions about the dipole orientation and intrinsic quantum efficiency need to be made.

The second process is the migration of the excitation energy inside the conjugated polymer. The occurrence of non-radiative energy transfer to the metal will lead to a gradient in the exciton population close to the metallic film. As a result, excitons will diffuse towards the metal interface, which increases the overall efficiency of the exciton quenching process. The exciton diffusion length in conjugated polymers, typically 5–10 nm,<sup>12,13</sup> is of the same order of magnitude as the estimates for the range of energy transfer to the metal. Therefore, a fundamental question to be solved is which of these two processes is mainly responsible for the quenching of excitons at metallic interfaces. In order to disentangle these two contributions, knowledge about the exciton migration dynamics, characterized by the exciton diffusion coefficient, is required. So far, the study of exciton diffusion in conjugated polymers has mainly been focused on the extraction of the exciton diffusion length  $L_D$ . In a recent study, we were able to extract both exciton diffusion coefficients and diffusion lengths from time-resolved PL measurements on a bilayer model system, consisting of PPV-based conjugated polymers and a polymerized fullerene.<sup>12,14,15</sup> In the present paper we analyze the dynamics of the quenching of excitons at metal interfaces by monitoring the time-resolved luminescence of a PPV-based conjugated polymer. Our knowledge of the exciton migration in the neat polymer enables us to disentangle the contributions from both the exciton diffusion and energy transfer to the metal, to the exciton quenching process.

In order to construct polymer/spacer layer/metal heterostructures (Fig. 1), poly2-(4-(3',7'-dimethyloctyloxy-phenyl))-co-2-methoxy-5-(3',7'-dimethyloctyloxy)-1,4-phenylene vinylene] (NRS-PPV), shown in Fig. 3, was spin coated from a toluene solution on top of the glass substrate under nitrogen atmosphere. Subsequently, thin transparent spacer layers of LiF were thermally evaporated on top of the

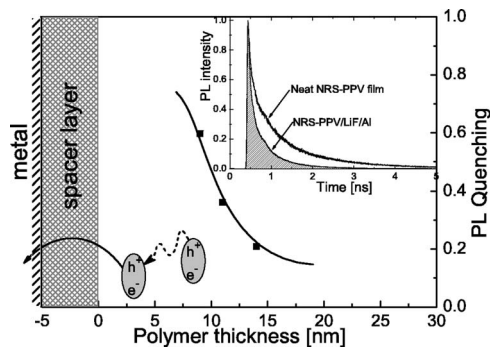


FIG. 1. PL quenching (■, right axis) in NRS-PPV/Li/Al structures vs polymer film thickness; the solid line is a guide to the eye. The relative quenching was derived by integration of the PL decay curves (inset). In the schematic diagram of the sample configuration exciton quenching is represented as a combination of diffusion and energy transfer to the metal.

polymer films and served as exciton blocking layers.<sup>16</sup> Finally, gold or aluminum layers were thermally evaporated on top of the spacer layers. Variation of the spacer layer thickness was employed to investigate the distance dependence of the nonradiative energy-transfer rate. First, time-resolved PL measurements were performed on NRS-PPV/LiF/aluminum heterostructures. LiF/Al films are widely used as cathodes in polymer photovoltaic cells and light-emitting diodes. The use of a LiF spacer layer has the advantage in that it prevents diffusion of metal atoms into the polymer layer. LiF layers of 5 and 100 nm of aluminum were thermally evaporated on top of NRS-PPV films with varying thicknesses. The polymer was excited with femtosecond laser pulses (200 fs) at 400 nm, and the luminescence was collected at its maximum, 580 nm. In these time-correlated single-photon counting (TCSPC) experiments<sup>17</sup> an instrument response function of 30 ps (full width at half maximum) was used for luminescence decay curve deconvolution. As a first step a comparison of the (time-integrated) areas under the PL decay curves for structures with and without metal interfaces provides a simple empirical measure for the efficiency of the PL quenching by the metal. As demonstrated before,<sup>3</sup> the dependence of the time-integrated PL on polymer thickness then provides a direct estimate of the width of the quenching zone at the polymer/metal interface. In Fig. 1 the relative time-integrated PL quenching<sup>12</sup> is plotted for various NRS-PPV film thicknesses. It appears that strong exciton quenching is observed within typically 15 nm from the Al/LiF interface. Note that this width is representative for the total exciton quenching process. As a next step we also investigated NRS-PPV/LiF/gold heterostructures; they are known to be chemically stable model systems with an efficient energy transfer. A normalized and deconvoluted luminescence decay curve of a 22-nm conjugated polymer film is depicted in Fig. 2, together with the reference luminescence decay curve of the neat polymer film. Upon the photoexcitation of the polymer excitons are formed. Their migration and nonradiative energy transfer to the metal result in a faster decay of the polymer luminescence. The LiF layer serves as a dielectric spacer and blocks excitons,<sup>16,18</sup> which allows study of the exciton quenching as a function of distance from the metal interface.

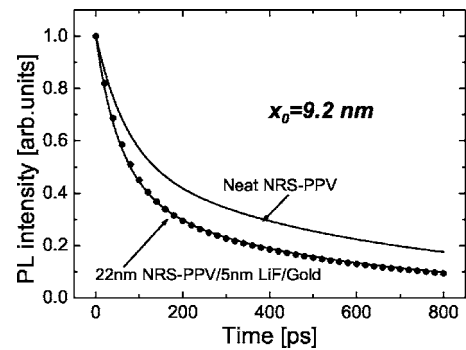


FIG. 2. Normalized luminescence decay curves for both the NRS-PPV/LiF/gold structure (●) and neat NRS-PPV as a reference (solid line). Simulation of these data by Eq. (3) with transfer range  $x_0$  as a fit parameter.

The exciton migration process is characterized by the exciton diffusion constant  $D$  and the exciton diffusion length  $L_D$ , which are related by

$$L_D = \sqrt{D\tau_\infty}, \quad (1)$$

where  $\tau_\infty$  is the exciton lifetime that accounts for the total process of radiative and nonradiative exciton decay. In a recent study an exciton diffusion coefficient of  $3 \times 10^{-4} \text{ cm}^2/\text{s}$  for NRS-PPV has been deduced.<sup>14</sup>

The distance ( $x$ ) dependence of the nonradiative decay rate constant  $r_{me}$  for organics in front of metal interfaces has been studied both experimentally<sup>19,20</sup> and theoretically,<sup>7</sup> where a general expression has been derived within classical light reflection theory. For the case of interest, corresponding to a small distance between emissive molecule and metal in comparison with the resonant wavelength, it can be approximated with a  $x^{-3}$  dependence<sup>7,21</sup>

$$r_{me} = \frac{1}{\tau_\infty} \frac{x_0^3}{x^3}, \quad (2)$$

where  $x_0$  is the characteristic distance of the energy transfer.

In order to model the time-resolved luminescence quenching in polymer/spacer/metal heterostructures and derive the transfer range  $x_0$  experimentally, we have combined the one-dimensional exciton diffusion equation for the photoexcitation energy distribution  $E(x,t)$  (Refs. 14 and 21) with Eq. (2),

$$\frac{\partial E(x,t)}{\partial t} = D \frac{\partial^2 E(x,t)}{\partial x^2} - \frac{E(x,t)}{\tau_\infty} \left[ 1 + \left( \frac{x_0}{x+th} \right)^3 \right] + g(x,t). \quad (3)$$

The spatial variable  $x$  represents the distance from the polymer/spacer interface. The first term on the right-hand side of Eq. (3) is the one-dimensional exciton diffusion, characterized by the diffusion coefficient  $D$ . In the second term, responsible for the decay of the exciton population, quenching by the metal is represented by a distance-dependent nonradiative energy-transfer subterm, where  $th$  stands for the thickness of the spacer layer. The last term describes the exciton generation process and is governed by the spatially

dependent absorption profile of the femtosecond laser pulse. The contribution of interference effects into the photogeneration profile is negligible in view of the small thicknesses of the polymer films under consideration. Thus an exponential distance dependence of the intensity of the excitation beam reflected from the metal interface is used for  $g(x, t)$ . The time dependence of this term is approximated by a delta function, as the excitation pulse width (200 fs) is short in comparison to the dynamics of the quenching. At both polymer film interfaces the boundary condition  $\partial E(x=L)/\partial x=0$  is applied, representing negligible surface quenching and the absence of exciton current on both boundaries. It should be noted that processing by spin coating implies that polymeric chains are mostly aligned in plane of the substrate. However, since exciton diffusion is mainly governed by interchain processes,<sup>22,23</sup> in-plane exciton diffusion is expected not to prevail. Therefore, a one-dimensional model gives a good approximation of the exciton migration process.

In general, when the emissive layer is separated from the metal by a dielectric layer (Fig. 1), the expression for the transfer rate in Eq. (2) and the corresponding term in Eq. (3) have to be modified due to the difference in dielectric constants. If the spacer dielectric constant is larger than the dielectric constant of the emissive layer, it is expected that the energy-transfer rate to the metal becomes smaller because of the suppression of the electrostatic interaction of an oscillating dipole with the metal. In our study, the intermediate dielectric layer of LiF has a similar dielectric constant ( $\epsilon_\infty \approx 2$ ) as the emissive conjugated polymer.<sup>24,25</sup> Therefore, a direct substitution of Eq. (2) into the diffusion equation can be made, extending the distance  $x$  from the polymer/spacer interface with the spacer thickness  $th$ .

$$r_{me} = \frac{1}{\tau_\infty} \left( \frac{x_0}{x + th} \right)^3. \quad (4)$$

To account for the exciton lifetime  $\tau_\infty$  the neat NRS-PPV film luminescence decay curve is recorded. A time-dependent exciton lifetime is used for analytical description of the nonmonoexponential luminescence decay.<sup>14</sup> Thus, the PL decay curve of the NRS-PPV/LiF/gold structure in Fig. 2 can now be numerically modeled by Eq. (3), with the neat polymer luminescence decay as a reference. The only fit parameter, the energy-transfer range  $x_0$ , is derived to be 9.2 nm for NRS-PPV film in front of a gold mirror with a 5-nm LiF spacer in between. Thus, the process of the energy transfer to the metal is disentangled from the exciton migration mechanism, which in turn can be spatially characterized by the exciton diffusion length,  $L_D \approx 6$  nm in pristine NRS-PPV films.<sup>12,14</sup>

In order to verify the  $x^{-3}$  distance dependence in our system and check the assumption made in Eq. (4), we have varied the thickness of the LiF spacer layer. PL decay curves analogous to Fig. 2 as a function of polymer film thickness were recorded for LiF exciton blocking layers varying from 3 to 13 nm in thickness. Analysis of these data with Eq. (3) provided the energy-transfer range  $x_0$  for polymer films at various distances from the quenching metal. When the distance dependence of the exciton quenching is correctly de-

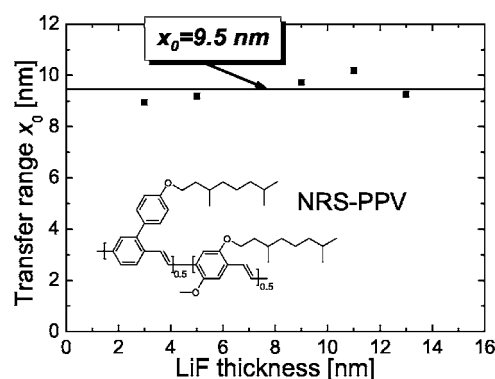


FIG. 3. Energy-transfer range  $x_0$  vs LiF spacer layer thickness in NRS-PPV/LiF/Au heterostructures. The inset shows the chemical structure of NRS-PPV.

scribed by Eq. (5), the parameter  $x_0$  should be independent on the geometry of the structure used. Indeed, as shown in Fig. 3,  $x_0$  was found to be independent on the spacer layer thickness  $th$  within the range studied;  $x_0$  only slightly fluctuates around an average number of 9.5 nm. This agreement proves the applicability of the inverse cubic distance dependence of the energy-transfer rate to the structures used in our study. Since the polymer film thickness is limited to only 35 nm, interference effects on the radiative lifetime can be excluded.<sup>3</sup>

Present polymer LEDs and photovoltaic devices often employ a cathode that consists of a thin LiF layer with aluminum evaporated on top.<sup>26,27</sup> Time-integrated PL quenching in NRS-PPV/LiF/Al heterostructures has been presented in Fig. 1. Subsequently, polymer luminescence decay curves were measured and, analogously to gold, analyzed in these structures for different thicknesses of a polymer film and constant thickness (5 nm) of the LiF spacer layer. In the inset of Fig. 4 luminescence decay curves are presented together with the fit to Eq. (3), which results in derivation of an energy-transfer range of 7.5 nm for the aluminum electrode. The reduction of the energy-transfer distance as compared to gold is predicted by theory<sup>7</sup> and is in qualitative agreement

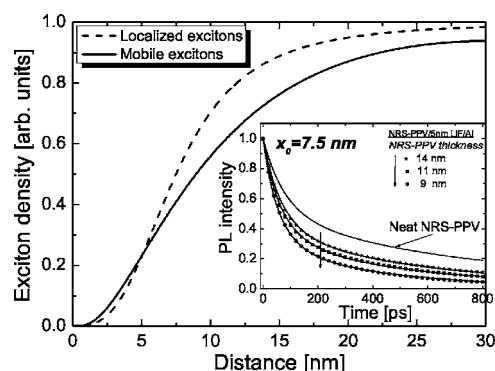


FIG. 4. Steady-state exciton density profiles simulated for NRS-PPV/Al heterostructures with experimentally determined values for  $x_0$  and  $D$ . The inset shows deconvoluted and normalized PL decay curves for NRS-PPV/LiF/Al structures for different polymer film thicknesses (symbols) with the simulation of these data by Eq. (3) with transfer range  $x_0=7.5$  nm (solid lines).

with the higher imaginary part of the complex refractive index of aluminum ( $K_2=6.33$ ) in comparison with gold ( $K_2=2.86$ ).<sup>28,29</sup> With the energy-transfer range  $x_0$  known we can simulate exciton density profiles at the polymer/Al interface, using  $x_0$  and  $D$  as input parameters. In this simulation steady-state uniform exciton generation is assumed to demonstrate the effect of exciton quenching in terms of energy transfer and exciton diffusion. Figure 4 shows the redistribution of the steady-state exciton density profile due to exciton migration for NRS-PPV/LiF/Al heterostructures. Compared to “localized” excitons ( $D=0$ ) the exciton population is shifted further away from the metal interface, due to the enhanced quenching. Furthermore, due to the diffusion-driven flow of excitons toward the metal interface, the exciton population at distances smaller than 5 nm exceeds the population of localized excitons. Relative quenching of mobile excitons estimated from areas under the curves in Fig. 4 for a 30-nm NRS-PPV film at an Al interface amounts to 38%, in contrast to 30% for virtually localized ones. Thus, the time-integrated relative quenching shown in Fig. 1 can now be quantitatively understood. The strong quenching, which is observed within a typical distance of 15 nm from the aluminum interface, is

due to the direct energy transfer to the metal with a characteristic distance of 7.5 nm, being further enhanced by an exciton density redistribution characterized by a diffusion length of 6 nm.

In summary, we have studied exciton quenching in conjugated polymer films due to the presence of a metal contact. Time-resolved PL measurements have been performed for characterization of this process. Nonradiative energy transfer is disentangled from the exciton migration process by the use of a diffusion-assisted energy-transfer model. The inverse cubic distance dependence of the energy-transfer rate has been demonstrated to be applicable to polymer/metal structures at distances of several tens of nanometers. Analysis of the luminescence decay curves resulted in typical energy-transfer ranges of 9.5 and 7.5 nm for gold and aluminum, respectively.

This work is a part of the research program of the Stichting voor Fundamenteel Onderzoek der Materie (FOM), financially supported by the Nederlandse Organisatie voor Wetenschappelijk Onderzoek (NWO).

- 
- <sup>1</sup>J. H. Burroughes, D. D. C. Bradley, A. R. Brown, R. N. Marks, K. Mackay, R. H. Friend, P. L. Burns, and A. B. Holmes, *Nature (London)* **347**, 539 (1990).
- <sup>2</sup>N. C. Greenham, S. C. Moratti, D. D. C. Bradley, R. H. Friend, and A. B. Holmes, *Nature (London)* **365**, 628 (1993).
- <sup>3</sup>H. Becker, S. E. Burns, and R. H. Friend, *Phys. Rev. B* **56**, 1893 (1997).
- <sup>4</sup>N. S. Sariciftci, *Prog. Quantum Electron.* **19**, 131 (1995).
- <sup>5</sup>C. J. Brabec, N. S. Sariciftci, and J. C. Hummelen, *Adv. Funct. Mater.* **11**, 15 (2001).
- <sup>6</sup>P. Peumans, V. Bulovic, and S. R. Forrest, *Appl. Phys. Lett.* **76**, 2650 (2000).
- <sup>7</sup>R. R. Chance, A. Prock, and R. Silbey, *J. Chem. Phys.* **62**, 2245 (1975).
- <sup>8</sup>K. H. Drexhage, in *Progress in Optics*, edited by E. Wolf (North-Holland, Amsterdam, 1974), pp. 163–232.
- <sup>9</sup>H. Kuhn, *J. Chem. Phys.* **53**, 101 (1970).
- <sup>10</sup>P. Avouris and B. N. J. Persson, *J. Phys. Chem.* **88**, 837 (1984).
- <sup>11</sup>R. R. Chance, A. H. Miller, A. Prock, and R. Silbey, *J. Chem. Phys.* **63**, 1589 (1975).
- <sup>12</sup>D. E. Markov, E. Amsterdam, P. W. M. Blom, A. B. Sieval, and J. C. Hummelen, *J. Phys. Chem. A* **109**, 5266 (2005).
- <sup>13</sup>J. J. M. Halls, K. Pichler, R. H. Friend, S. C. Moratti, and A. B. Holmes, *Appl. Phys. Lett.* **68**, 3120 (1996).
- <sup>14</sup>D. E. Markov, J. C. Hummelen, P. W. M. Blom, and A. B. Sieval, *Phys. Rev. B* **72**, 045216 (2005).
- <sup>15</sup>D. E. Markov, C. Tanase, P. W. M. Blom, and J. Wildeman, *Phys. Rev. B* **72**, 045217 (2005).
- <sup>16</sup>K. G. Sullivan, O. King, C. Sigg, and D. G. Hall, *Appl. Opt.* **33**, 2447 (1994).
- <sup>17</sup>J. N. Demas, *Excited State Lifetime Measurements* (Academic, New York, 1983).
- <sup>18</sup>W. R. Holland and D. G. Hall, *Phys. Rev. Lett.* **52**, 1041 (1984).
- <sup>19</sup>G. Vaubel, H. Baessler, and D. Mobius, *Chem. Phys. Lett.* **10**, 334 (1971).
- <sup>20</sup>G. Cnossen, K. E. Drabe, and D. A. Wiersma, *J. Chem. Phys.* **98**, 5276 (1993).
- <sup>21</sup>A. L. Burin and M. A. Ratner, *J. Phys. Chem. A* **104**, 4704 (2000).
- <sup>22</sup>B. J. Schwartz, *Annu. Rev. Phys. Chem.* **54**, 141 (2003).
- <sup>23</sup>T. Q. Nguyen, J. J. Wu, V. Doan, B. J. Schwartz, and S. H. Tolbert, *Science* **288**, 652 (2000).
- <sup>24</sup>H. C. F. Martens, H. B. Brom, and P. W. M. Blom, *Phys. Rev. B* **60**, R8489 (1999).
- <sup>25</sup>F. Bernardini and V. Fiorentini, *Phys. Rev. B* **58**, 15292 (1998).
- <sup>26</sup>J. Yoon, J. J. Kim, T. W. Lee, and O. O. Park, *Appl. Phys. Lett.* **76**, 2152 (2000).
- <sup>27</sup>V. D. Mihailetschi, L. J. A. Koster, and P. W. M. Blom, *Appl. Phys. Lett.* **85**, 970 (2004).
- <sup>28</sup>P. B. Johnson and R. W. Christy, *Phys. Rev. B* **6**, 4370 (1972).
- <sup>29</sup>G. Hass and J. E. Waylonis, *J. Opt. Soc. Am.* **51**, 719 (1961).